NDT&E International 59 (2013) 34–39

Contents lists available at SciVerse ScienceDirect

NDT&E International

journal homepage: www.elsevier.com/locate/ndteint

Non-destructive microwave evaluation of plasma sprayed TBCs porosity

Yu'e Yang [a,b], Cunfu He [a,*], Bin Wu [a]

[a] College of Mechanical Engineering and Applied Electronics Technology, Beijing University of Technology, Beijing 100124, China
[b] Physics and Information Engineering Department, Jining University, Qufu, Shandong 273155, China

ARTICLE INFO

Article history:
Received 11 December 2012
Received in revised form
27 April 2013
Accepted 28 April 2013
Available online 6 May 2013

Keywords:
Microwave non-destructive evaluation
Thermal barrier coatings
Porosity
Reflected coefficient

ABSTRACT

Porosity of top coating (TC) in thermal barrier coatings (TBCs) is one of the main factors affecting the thermal conductivity and causing failure of TBCs. To ensure the quality of the TBCs, the evaluation of TC porosity was carried out using a microwave non destructive technique. The reflection coefficient at the interface of TC and waveguide probe was studied with regard to the TC porosity using computer simulation technology-microwave studio (CST-MWS). The results showed that the greater the porosity of the TC the larger the phase difference when the microwave was operated at the sensitive frequency. And the sensitive frequency is different when TC thickness changes. Besides, a network analyzer was used to measure the reflection coefficient phase which can be used in the evaluation of the TC porosity. The results showed that the phase difference increases linearly with increasing porosity of TC when the network analyzer operating over the frequency range of 30 GHz to 40 GHz. Therefore, the porosity of TC can be calculated by measuring the phase of the reflection coefficient. The experimental results are consistent with the theory simulation ones.

Crown Copyright © 2013 Published by Elsevier Ltd. All rights reserved.

1. Introduction

Thermal barrier coatings (TBCs) are currently used for heat insulation in high-temperature and high-pressure gas engine components to increase efficiency. TBCs consists of a metallic bond coating (BC) deposited directly onto the substrate metal surface followed by the application of a ceramic top coating (TC), which is usually yttria-stabillized zirconia (YSZ). TBCs failure attributed by the bond coating oxidation and top coating degradation [1] will result in rapid substrate material degradation. The TC porosity influences the TBCs characterization including the thermal conductivity and the global stiffness [2–4]. If the TC porosity increases, the elastic modulus decreases and the compressive stress near the surface decrease [5], which affect top coating degradation. Besides, the independent study into the relationship between air plasma sprayed (APS) coating porosity and thermal conductivity showed the trend with respect to decreasing thermal conductivity with increasing porosity [6]. And it is known that such factors as pore orientation, in addition to pore fraction, influence the thermal conductivity of a coating [7]. Air plasma sprayed TBCs usually include lamellar structure with high interconnected porosities, which is because that the spraying parameters influence the coating morphology and porosity level [8,9].

Various nondestructive techniques have been developed for evaluation of TC porosity including mercury porosimetry [10,11], electrochemical impedance spectroscopy [12,13], impedance Spectroscopy [14], ultrasonic and capacitance techniques [15], cathode luminescence (CL) spectroscopy [16], ultrasonic leaky surface wave technique [17], metallographic techniques and digital image analysis [18]. Accurate information on TC porosity is highly desirable particularly when evaluating a kind of new air plasma spraying technological process or when process parameters have changed. However, rapid evaluation is difficult using conventional non-destructive techniques.

Although not as widely known or understood as other non-destructive evaluation techniques, microwave non-destructive evaluation (NDE) has proven to be very useful in certain applications including detection of delamination in IC packages[19,20] , detection of disbands or thickness in dielectric joints[21–24], detection of cracks on metal surfaces[25–28]. Non-contact inspection and the ability to penetrate into dielectric materials are two of the most important attributes of microwave NDE and make it suitable for the non-destructive inspection of TBCs. The thickness of TBCs, defects on substrate interface, cracks and pores of TC can be easily visualized using microwave scanning probe [29]. The phase and magnitude of the microwave reflection coefficient can evaluate the TBCs delamination induced by acute angle laser drilling using microwave NDE [30]. The phase difference of microwave reflection coefficient can be used to evaluate the thickness of TC and thermal growth oxide (TGO) in TBCs

* Corresponding author.
E-mail address: hecunfu@bjut.edu.cn (C. He).

0963-8695/$ - see front matter Crown Copyright © 2013 Published by Elsevier Ltd. All rights reserved.
http://dx.doi.org/10.1016/j.ndteint.2013.04.010

using microwave NDE operating over K- and W-band frequency range [31].

TC porosity was different when a kind of new air plasma spraying technological process was applied or when process parameters have changed. So, it is very important to evaluate TC porosity using microwave NDE. In this study, changes in the phase of reflection coefficient were primarily studied to represent TC porosity. Firstly, the frequency, used in Microwave NDE, was optimized according to TC thickness using computer simulation technology-microwave studio (CST-MWS). And then, the appropriate rectangular waveguide was used to evaluate TC porosity according to the optimization results. The objective of this study is to investigate feasibility of microwave NDE to evaluate TC porosity.

2. Theoretical bases

The problem of transmission and reflection of uniform plane waves from a multilayer dielectric medium has been investigated by many investigators. This microwave NDE is based on wave reflection from a dielectric media interface. Metallic BC thickness does not affect microwave signals, so, in this case, TC was deposited directly onto the metal substrate. Uniform waves were normally incident into the TC system and then reflected by the metal surface (good conductor layer). These forward- and backward-traveling waves inside the TC layer were formulated by enforcing the appropriate boundary conditions at the air-TC and TC-conductor boundaries. Finally, the reflection coefficient was set as the ratio of the reflected and incident waves [32]. Fig. 1 shows the incident and reflected electric fields traveling in TC systems.

The incident electric fields of the probe, $E_0^i(\mathrm{Vm}^{-1})$, that incident into TC system, E_{TC}^i and that reflected by the metal surface, E_{TC}^r. After being completely reflected by the TC and substrate, the field emerged as a reflected electric field in the probe, E_0^r. The reflection coefficient is the ratio of E_0^r and E_0^i. The reflection coefficient Γ and its phase ϕ at the sensor aperture can be written as follows:

$$\Gamma = \frac{E_0^r}{E_0^i} = \frac{\eta_{TC}^{'} - \eta_0}{\eta_{TC}^{'} + \eta_0}$$

$$\phi = \tan^{-1}\left[\frac{\mathrm{Im}(\Gamma)}{\mathrm{Re}(\Gamma)}\right] \quad (1)$$

Where

$$\eta_{TC}^{'} = \eta_{TC}\frac{1+\Gamma_1^{'}}{1-\Gamma_1^{'}} \quad (2)$$

$$\Gamma_1^{'} = \frac{E_{TC}^r}{E_{TC}^i} = \exp(-j2k_{TC}d_{TC})\Gamma_1 \quad (3)$$

$$\Gamma_1 = -1 \quad (4)$$

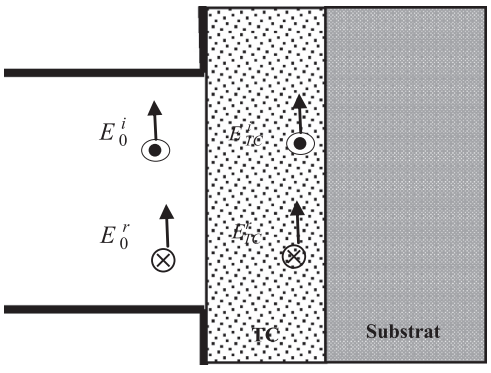

Fig. 1. Incident and reflected electric fields traveling in TC systems consisting of a rectangular waveguide probe and TC backed by a conducting metallic substrate.

$$k_{TC} = \omega\sqrt{\mu_{TC}\varepsilon_{eTC}} \quad (5)$$

$$\eta_{TC} = \sqrt{\frac{\mu_{TC}}{\varepsilon_{eTC}}} \quad (6)$$

Γ is the reflection coefficient at sensor aperture. Γ_1 is the reflection coefficient at the interface of TC and substrate. η_0 is the characteristic impedance of the medium in the waveguide. η_{TC} is the characteristic impedance of TC. η'_{TC} is the equivalent impedance of TC in metallic substrate. k_{TC}, d_{TC}, μ_{TC} and ε_{TC} are the phase constant, thickness, magnetic permeability and permittivity of TC, respectively.

When microwave signals travel within TC systems, the permittivity of the TC affect the phase constant and the characteristic impedance, thereby affecting the reflection coefficient. TC permittivity decreases as TC porosity increases [33]. L. Gao and J. Z. Gu investigated the effective dielectric constant of a two-component material and obtained three formulas to calculate the effective dielectric constant [34]:

$$\varepsilon_{eTC} = \varepsilon_2\frac{1+\theta(\sqrt{\varepsilon_1/\varepsilon_2}-1)}{1+\theta(\sqrt{\varepsilon_2/\varepsilon_1}-1)} \quad (7)$$

$$\varepsilon_{eTC} = [\theta\varepsilon_1^{-1/2} + (1-\theta)\varepsilon_2^{-1/2}]^{-2} \quad (8)$$

$$\varepsilon_{eTC} = \varepsilon_2\left[\frac{1+\theta+\sqrt{\varepsilon_2/\varepsilon_1}(1-\theta)}{1-\theta+\sqrt{\varepsilon_2/\varepsilon_1}(1+\theta)}\right]^2 \quad (9)$$

θ is the porosity of the TC, and ε_{eTC} and ε_2 are the effective permittivity of TC with and without pores respectively. ε_1 is the permittivity of pores.

Eq. (7) is regarded as the Maxwell–Garnett-type approximation including the shape distribution (SDMGA). Eq. (8) is regarded as the Bruggeman-type effective medium approximation with the shape distribution (SDEMA). Eq. (9) is the differential effective medium approximation with shape distribution (SDDEMA).

According to above formulas, effective dielectric constant ε_{eTC} becomes smaller, when porosity θ increases. And effective dielectric constant affect microwave reflection coefficient Γ. Therefore TC porosity dependent on TC effective dielectric constant can be characterized by the reflection coefficient. In order to find the best working frequency detecting TC porosity, the reflection coefficient at the interface of TC and waveguide probe was studied using computer simulation technology-microwave studio (CST-MWS) in different frequency range. And, an Agilent E8363C network analyzer was used to measure the amplitude and phase variations of reflection coefficient with regard to the TC porosity.

3. Parameters optimization using CST-microwave studio

CST-MWS is a specialized tool for the 3D electromagnetism (EM) simulation of high-frequency components. The reflection coefficient at the interface of TC and waveguide probe was studied with regard to the TC porosity using computer simulation technology-microwave studio. Contact evaluation was used to evaluate TC porosity using rectangular waveguide probe. Three probes WR42, WR28 and WR18 were used. Fig. 2(a) shows the cross section of WR42 or WR28. Fig. 2(b) shows the cross section of WR18. Table 1 shows the size of the probes. Perfect electric conductors 100 mm width, 100 mm in length, and 4 mm in thickness were used as substrates in this study.

In order to limit the influence of TC thickness, the thicknesses of TC in one group was kept the same during the evaluation of TC porosity. When the phase differences were calculated, the reflection coefficient phase of TC with 3% porosity was set as the benchmark. Thus, the phase difference for cases of other porosities

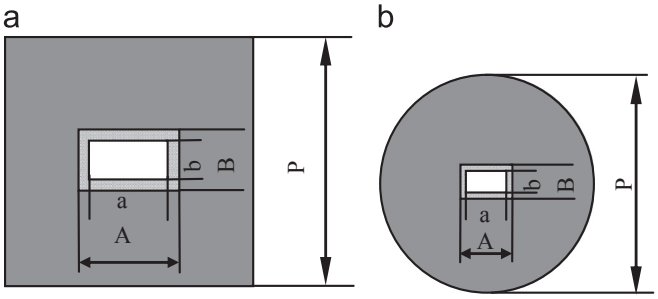

Fig. 2. Cross sections of rectangular waveguide probes (a) WR42 or WR28, (b) WR18.

Table 1
Type and size of rectangular waveguide probes.

Probe model	a (mm)	A (mm)	b (mm)	B (mm)	P (mm)
WR42	10.668	12.7	4.318	6.35	22.4
WR28	7.112	9.14	3.556	5.59	19.1
WR18	4.775	6.81	2.338	4.42	28

relative to 3% porosity can now be measured for various TC thicknesses and microwave frequencies. The phase difference was calculated for TC of 10% relative to 3% porosity when TC thickness was kept constant within one group to limit its influence. Fig. 3 shows the phase difference vs. frequency using three probes, WR18, WR28, and WR42. The results show that there is the maximum phase difference in each phase difference curve and that TC thickness was equal to one quarter of the wavelength of the microwave when the microwave operated at the frequency corresponding to the maximum phase difference, which is called the sensitive frequency. Thus, under actual testing conditions, TC porosity was able to be determined using this microwave technique by selecting the appropriate frequency, which was estimated according to TC thickness. Once this was known, the appropriate waveguide probe can be selected. The phase difference of the microwave reflection coefficient indicated TC porosity using probe WR18 when TC thickness was 300 to 350 μm, using probe WR28 when TC thickness was 400 to 550 μm, and using probe WR42 when TC thickness was 700 to 900 μm.

4. Experimental procedure

4.1. Sample preparation

Inconel 625 alloy (58Ni-21.5Cr-9Mo-5Fe-3.75Nb) with the dimension of 100 mm width, 100 mm length and 4 mm in thickness were used as substrate in this study. Each of specimens consists of a 400 ± 5 μm thick yttria stabilized zirconia (YSZ, Amperit-No 827.054, H. C. Starck, made in Germany) as TC deposited directly on the substrate metal by air plasma spraying (APS). Table 2 shows three groups of APS parameters in order to produce three kinds of TCs with different porosity. Fig. 4 show the micrographs of TCs in different APS parameters. Fig. 4(a) shows micrograph of TC coated by the first group APS parameters in Table 2. Fig. 4(b) shows micrograph of TC coated by the second group APS parameters in Table 2. Fig. 4(c) shows micrograph of TC coated by the third group APS parameters in Table 2. The porosities of TCs coated by different APS parameters were obtained using digital image analysis. In the first group, the porosity of TC is $3.00\% \pm 0.47\%$, average pore size is 9.5 μm^2, pore surface density is 3158 per square millimeter. In the second group, the porosity of TC is $8.18\% \pm 0.94\%$, average pore size is 22.8 μm^2,

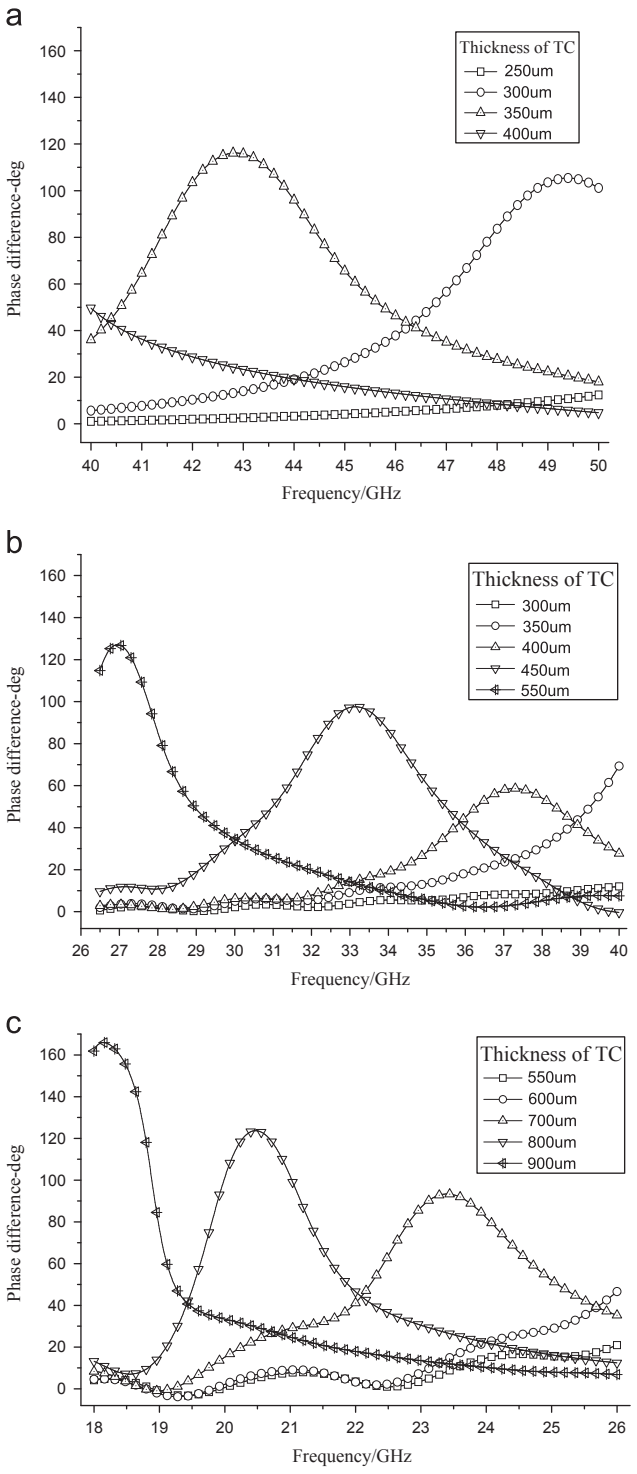

Fig. 3. Phase differences of 10% relative to 3% TC detected by (a) WR18, (b) WR28, and (c) WR42 probe for TC of different thicknesses.

Table 2
Tree groups of APS parameters in order to produce three kinds of TCs with different porosity.

	Argon flow (l/min)	Hydrogen flow (l/min)	Current (A)	Spray distance (mm)	Preheat temperature (°C)	Powder feed rate (g/min)
1	45	11	600	65	250	30
2	32	8	550	90	400	30
3	32	8	550	120	250	30

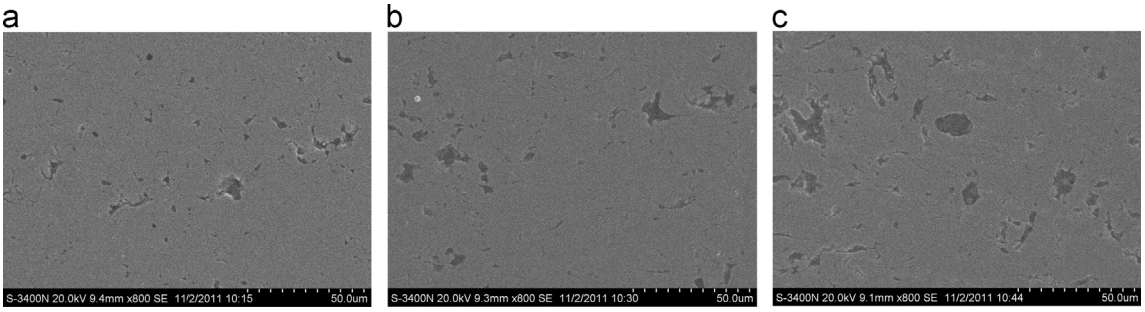

Fig. 4. Micrographs of TC in different APS parameters: (a) the spay distance is 65 mm, (b) the spay distance is 90 mm, (c) the spay distance is 120 mm.

pore surface density is 2632 per square millimeter. In the third group, the porosity of TC is 10.0% ± 1.8%, average pore size is 36.0 μm^2, pore surface density is 2778 per square millimeter.

4.2. Microwave non-destructive evaluation

According to the theoretical results, the phase difference of the microwave reflection coefficient can indicate TC porosity using probe WR28 (26.5–40 GHz) when TC thickness was 400 to 550 μm. So, the measurement system used in this study consisted of a network analyzer (Agilent E8363C, 10 MHz–40 GHz) feeding signals to a Ka-band (26.5–40 GHz) rectangular waveguide (Agilent R281A). This waveguide was used as a sensor here to both transmit and receive signals from specimens. An in-contact inspection technique was applied for detecting and evaluating the TC porosity. Fig. 5 shows the test equipment of evaluating TC porosity using microwave non-destructive evaluation.

5. Results and discussion

To evaluate TC porosity, the phase and phase difference of the reflection coefficient were studied. The reflection coefficient phase was measured directly by network analyzer. The phase difference for cases with TC porosity in θ and in 3% can now be calculated:

$$\Delta\phi = \phi_\theta - \phi_{3\%} \tag{10}$$

θ is the TC porosity. $\Delta\phi$, ϕ_θ and $\phi_{3\%}$ are the phase difference, the microwave phase of detecting TC in θ porosity and the microwave phase of detecting TC in 3% porosity, respectively.

5.1. Phase to characterize TC porosity

In order to limit the influence of TC thickness, the thicknesses of TC was kept the same during the evaluation of TC porosity. Fig. 6 shows the experimental and simulation results of reflection coefficient phase according to microwave frequency for three cases of 3%, 8% and 10% porosity of TC.

The results show that the reflection coefficient phase decreases with increasing microwave frequency when evaluate same specimen. This may be primarily attributed to that the microwave wavelength in TC decreases when the operating frequency increases. Besides, the results indicate the phase increases with increasing porosity when operating over the frequency range of 30 GHz to 40 GHz. So, the reflection coefficient phase can characterize the TC porosity. The results indicate good agreement between the experimental and simulation data. The deviation from the simulation result can be attributed to inaccurate knowledge of the TC permittivity and non-ideal contact between TC and waveguide in experiment, because there is a certain roughness of the TC surface.

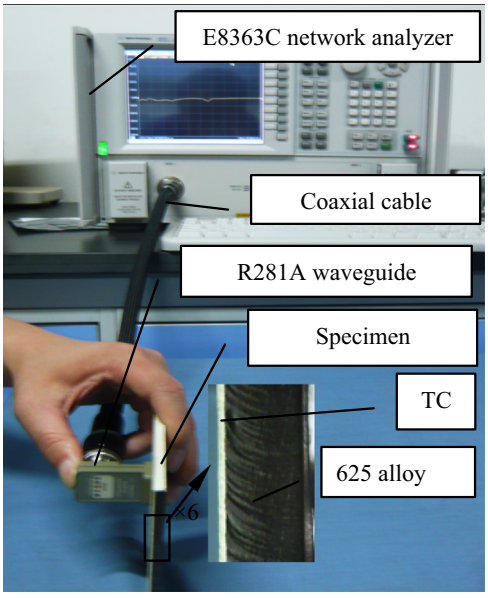

Fig. 5. The test equipment of evaluating TC porosity using microwave non-destructive evaluation.

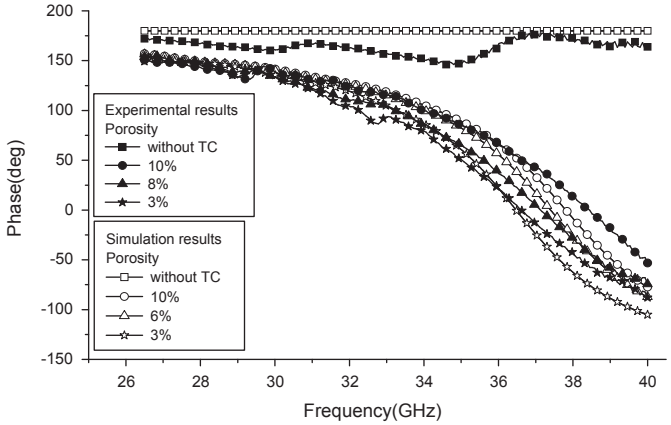

Fig. 6. Experimental and theoretical results of reflection coefficient phase according to microwave frequency for three cases of 3%, 8% and 10% porosity of TC.

Fig. 7 shows the experimental results of reflection coefficient phase as a function of TC porosity.

The results show that the reflection coefficient phase is larger in high porosity than in low porosity. The main reason is that TC permittivity decreases as TC porosity increases [32]. The results show a good linear relationship between the reflection coefficient phase and the TC porosity:

$$\phi = A\theta + B \tag{11}$$

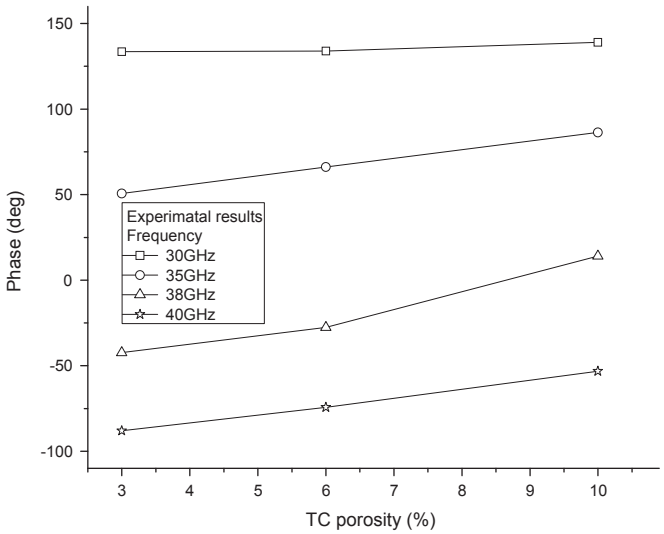

Fig. 7. Experimental results of reflection coefficient phase as a function of TC porosity.

Table 3
The values of the coefficients (A, B) in four operating frequencies.

	30 GHz	35 GHz	38 GHz	40 GHz
A	80.69	509.61	817.24	500.36
B	131.97	45.61	−54.04	−93.53

ϕ is the reflection coefficient phase, θ is the TC porosity, A and B are the coefficients which vary when operating frequency changes. Table 3 shows the values of the coefficients (A, B) in four different operating frequencies. The results show a resolution of about 0.8°, 5°, 8° and 5° change in phase for 1% TC porosity when operating frequency is 30 GHz, 35 GHz, 38 GHz and 40 GHz, respectively. Therefore, it is feasible to evaluate TC porosity by reflection coefficient phase using microwave NDE.

5.2. Phase difference to characterize TC porosity

In addition to the reflection coefficient phase to characterize TC porosity, the phase difference of the reflection coefficient, which is calculated by formula (10), can be used to evaluate TC porosity. Fig. 8 shows the experimental and simulation results of reflection coefficient phase difference according to microwave frequency for two cases of 8% and 10% porosity of TC. The results indicate that the phase difference change is strongly dependent on frequency and TC porosity. In the frequency range of 30 GHz to 40 GHz, the phase difference increases with increasing TC porosity. And for the frequency range of 37.5 GHz to 38.5 GHz, which were called sensitive frequency, phase difference is more sensitive to TC porosity than for others. The results indicate good agreement between the experimental and simulation data. The deviation from the simulation result can be attributed to inaccurate knowledge of the TC permittivity and non-ideal contact between TC and waveguide in experiment.

Fig. 9 shows the experimental results of reflection coefficient phase difference according to TC porosity. The results show that the phase difference increases with increasing of the TC porosity, but not linearly. When the TC porosity increases from 8% to 10%, the phase difference has a greatest change operating in 38 GHz frequency. The results indicate a maximum phase difference of approximately 56° for 10% porosity TC at 38 GHz.

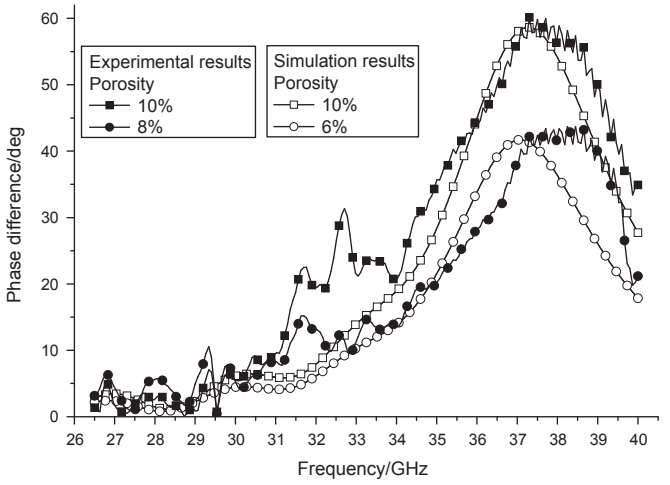

Fig. 8. Experimental and theoretical results of reflection coefficient phase difference according to microwave frequency for two cases of 8% and 10% porosity of TC.

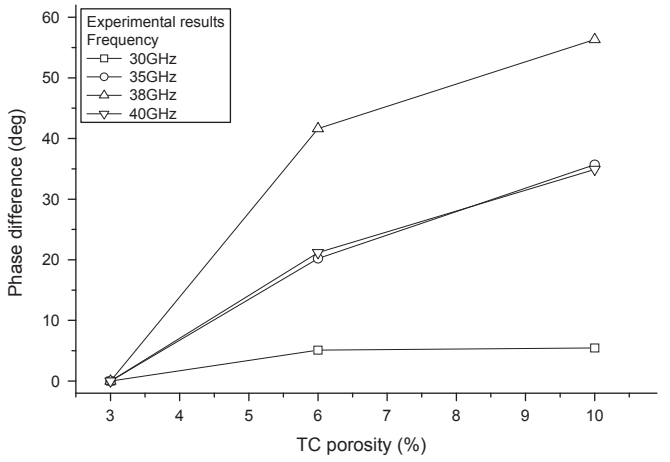

Fig. 9. Experimental results of reflection coefficient phase difference according to TC porosity.

6. Conclusions

Microwave NDE of TC porosity has been carried out in this study. CST-MWS was used to calculate the relation of phase difference (with prospect to a non-porosity case) vs. frequency according to various TC thicknesses. The results show that the sensitive frequency is different when TC thickness changes.

An Agilent E8363C network analyzer was used to measure the phase variations of reflection coefficient when TC thickness is 400 μm. According to the calculated results, the sensitive frequency is about 37.5 GHz. So, the open-ended rectangular waveguide-R281A was used as a sensor to both transmit and receive signals from TC. Two methods were used to evaluate TC porosity. The first one was to characterize the TC porosity using the reflected coefficient phase. The second method was to calculate the phase difference of the reflection coefficient between 3% porosity TC and others. In the first method, the results show that the phase increases with increasing porosity when operating over the frequency range of 30 GHz to 40 GHz. So, the reflection coefficient phase can characterize the TC porosity. In the second method, the results show that the phase difference increases with increasing of the TC porosity, and a maximum phase difference of approximately 56° for 10% porosity TC at 38 GHz. Therefore, it is feasible to evaluate the TC porosity using non-destructive

microwave evaluation. However, it is necessary to choose appropriate operating frequency according to TC thickness.

Acknowledgements

This project is supported by the National Natural Science Foundation of China under contract 11072010 and the National Natural Science Foundation (Special Foundation) of China under contracts 10827201.

References

[1] Chen WR, Wu X, Marple BR, Patnaik PC. The growth and influence of thermally grown oxide in a thermal barrier coating. Surf Coat Technol 2006;201:1074–9.
[2] Cernuschi F, Bison PG, Marinetti S, Scardi P. Thermophysical, mechanical and microstructural characterization of aged free-standing plasma-sprayed zirconia coatings. Acta Mater 2008;56:4477–88.
[3] Paul S. Assessing coating reliability through pore architecture evaluation. J Therm Spray Technol 2010;19(4):779–86.
[4] Curry Nicholas, Markocsan Nicolaie, Li Xin-Hai, Tricoire Aurélien, Dorfman Mitch. Next generation thermal barrier coatings for the gas turbine industry. J Therm Spray Technol 2011;20(1-2):108–15.
[5] Teixeira Vasco. Numerical analysis of the influence of coating porosity and substrate elastic properties on the residual stresses in high temperature graded coatings. Surf Coat Technol 2001;146–147:79–84.
[6] Bertrand Ghislaine, Bertrand Pierre, Roy Priscille, Rio Catherine, Mevrel Rémy. Low conductivity plasma sprayed thermal barrier coating using hollow psz spheres: Correlation between thermophysical properties and microstructure. Surf Coat Technol 2008;202(10):1994–2001.
[7] Lu Tian Jian, Levi Carlos G, Wadley Haydn NG, Evans Anthony G. Distributed porosity as a control parameter for oxide thermal barriers made by physical vapor deposition. J Am Ceram Soc 2001;84(12):2937–46.
[8] Markocsan N, Nylén P, Wigren J, Li X-H. Low thermal conductivity coatings for gas turbine applications. J Therm Spray Technol 2007;16(4):498–505.
[9] Saremi Mohsen, Afrasiabi Abbas, Kobayashi Akira. Microstructural analysis of YSZ and YSZ/Al2O3 plasma sprayed thermal barrier coatings after high temperature oxidation. Surf Coat Technol 2008;202:3233–8.
[10] Furke C, Mailand JC, Siebert B, Vaβen R, Stöver D. Characterization of Zr02-7 wt % YsO3 thermal barrier coatings with different porosities and FEM analysis of stress redistribution during thermal cycling of TBCs. Surf Coat Technol 1997;94–95:106–11.
[11] Portinha A, Teixeira V, Carneiro J, Martins J, Costa MF, Vassen R, et al. Characterization of thermal barrier coatings with a gradient in porosity. Surf Coat Technol 2005;195:245–51.
[12] Zhang J, Desai V. Evaluation of thickness, porosity and pore shape of plasma sprayed TBC by electrochemical impedance spectroscopy. Surf Coat Technol 2005;190(1):98–109.
[13] Jayaraj B, Desai VH, Lee CK, Sohn YH. Electrochemical impedance spectroscopy of porous ZrO2–8 wt% Y2O3 and thermally grown oxide on nickel aluminide. Mater Sci Eng, A 2004;A372(1–2):278–86.
[14] Yang Fan, Xiao Ping. Nondestructive evaluation of thermal barrier coatings using impedance spectroscopy. Int J Appl Ceram Technol 2009;6(3):381–99.
[15] Rogé B, Fahr A, Giguère JSR, McRae KI. Nondestructive measurement of porosity in thermal barrier coatings. J Therm Spray Technol 2003;12(4):530–5.
[16] Mauer Georg, Sebold Doris, Vaβen Robert, Stöver Detlev. Characterization of plasma-sprayed Yttria-stabilized zirconia coatings by cathodoluminescence. J Therm Spray Technol 2009;18(4):572–7.
[17] Fahr A, Giguère JSR, Rogé B, McRae KI. Application of NJJE in aerospace coatings. Int Soc Opt Eng 2002;4702:83–92.
[18] Kelly Matthew, Singh Jogender, Todd Judith, Copley Steven, Wolfe Douglas. Metallographic techniques for evaluation of thermal barrier coatings produced by electron beam physical vapor deposition. Mater Charact 2008;59:863–70.
[19] Ju Y, Saka M, Abé H. Microwave nondestructive detection of delamination in IC packages utilizing open-ended coaxial line sensor. NDT & E 1999;32:259–64.
[20] Ju Y, Saka M. Detection of delamination in IC packages using the phase of microwaves. NDT and E Int 2001;34:49–56.
[21] Abou-Khousa Mohamed, Zoughi R. Disbond thickness evaluation employing multiple-frequency near-field microwave measurements. IEEE Trans Instrum Meas 2007;56(4):1107–33.
[22] Kharkovsky Sergey, Nanni Emilio, Zoughi Reza. Application of frustrated total internal reflection of millimeter waves for detection and evaluation of disbands in dielectric joints. Appl Phys Lett 2008;92 094101-1-3.
[23] Kharkovsky Sergey, Nanni Emilio, Zoughi Reza. Application of frustrated total internal reflection of millimeter waves for detection and evaluation of disbonds in dielectric joints. Appl Phys Lett 2008;92(9)094101-(1-3).
[24] Ghasr MT, Simms Devin, Zoughi R. Multimodal solution for a waveguide radiating into multilayered structures-dielectric property and thickness evaluation. IEEE Trans Instrum Meas 2009;58(5):1505–13.
[25] Kerouedan Julien, Qu´eff´elec Patrick, Talbot Philippe, Quendo C´edric, De Blasi1 Serge, Le Brun Alain. Detection of micro-cracks on metal surfaces using near-field microwave dual-behavior resonator filters. Meas Sci Technol 2008;19(10):105701–10.
[26] Zoughi R, Kharkovsky S. Microwave and millimetre wave sensors for crack detection. Fatigue Fract Eng Mater Struct 2008;31:695–713.
[27] Li Yong, Tian Gui Yun, Bowring Nick, Rezgui Nacer. A microwave measurement system for metallic object detection using swept-frequency radar. Int Soc Opt Eng 2008;7117(13) 71170K-1-71170K-13.
[28] Ju Yang, Liu Linsheng, Ishikawa M. Quantitative evaluation of wall thinning of metal pipes by microwaves. Mater Sci Forum 2009;614:111–6.
[29] Grishin AM, Denysenkov VP. Broad band microwave probe for nondestructive test of dielectric coatings. IEEE Int Symp Appl Ferroelectr 2002:91–3.
[30] Sezer HK, Li Lin, Wu Z, Anderson B, Williams P. Non-destructive microwave evaluation of TBC delamination induced by acute angle laser drilling. Meas Sci Technol 2007;18(1):167–75.
[31] Sayar M, Seo D, Ogawa K. Non-destructive microwave detection of layer thickness in degraded thermal barrier coatings using K- and W-band frequency range. NDT and E Int 2009;42(5):398–403.
[32] Edwards J, Zoughi R. Microwave sensitivity maximization of disbond characterization in conductor backed dielectric composites. J Nondestr Eval 1993;12(3):193–8.
[33] Gerhardt R. Characterization of porosity in thermal barrier coating. ceramic thin and thick films. Wester-ville, OH: American Chemical Society; 189–99.
[34] Gao L, Gu JZ. Effective dielectric constant of a two-component material with shape distribution. J Phys D: Appl Phys 2002;35:267–71.